NUMERICAL INVESTIGATION OF THE CHARACTERISTICS OF RADIANT HEAT TRANSFER IN A TURBINE GRID

E. N. Bogomolov and V. I. Orlova

UDC 621.438:536.24

The Monte Carlo method is used to investigate the distribution of radiant heat fluxes in the interblade channel of a turbine grid and directionality diagram of the emitted radiation.

In designing turbine blades, the high temperature level of the basic working body that is typical of modern gas-turbine motors means that it is necessary to take account of the radiative heat transfer in the grid, due mainly to the radiant heat flux originating from the combustion zone in the combustion chamber (the emission of the medium in the turbine itself may usually be neglected, since, as shown by calculations based on the known experimental data [1, 2], it is approximately an order of magnitude smaller than the emission of the burning gas). The influence of the radiant heat flux incident at the grid is found to be especially significant in the presence of film cooling of the blade surface, which is becoming steadily more widely used in gas turbines. Reduction in efficiency of blade cooling $\theta = (T_G^* - T_B^*)/(T_G^* - T_A^*)$ under the influence of the radiant heat flux may only be compensated by intensification of the internal convective cooling of the blade, whereas the use of film cooling is practically associated with attenuation of the convective heat transfer on account of redistribution of the coolant flow rates. According to heat balance, this reduction in cooling efficiency is

$$\Delta\theta = (1-\theta_{conv})\bar{E}_B = \frac{1-\theta_0}{1-\theta_F}\bar{E}_B, \tag{1}$$

where

$$\bar{E}_B = E_B/[\alpha_G(T_G^* - T_A^*)]. \tag{2}$$

In the present work, the laws of radiant heat transfer are studied using the Monte Carlo method for the example of a parabolic grid, typical for the solar apparatus of gas turbines. Account is taken here of external radiation and the surface emission of the blades, while the emission of the medium in the grid is regarded as insignificant.

Suppose that the convex and concave surfaces of the interblade channel in the grid are described by the equations

$$y_S = A_S x_S^2 + B_S x_S, \tag{3}$$

$$y_b = A_b x_b^2 + B_b x_b + C_b, \tag{4}$$

and the ordinate is directed along the front of the grid (Fig. 1). Assume that, in the general case, the boundary of the interblade channel (including the outline of the inlet OG and the outlet EF) has intrinsic emission directed within the region OEFGO. To solve the problem of the distribution of radiant energy absorbed by the boundaries of the isolated region, the Monte Carlo method is used [3, 4], assuming that the boundaries OG and EF each consist of n sections and the boundaries OE and GF each of m sections; in unit time, any of these emit N portions of energy, propagating in the plane of the interblade-channel cross section over a rectilinear trajectory in the transparent medium.

Translated from Inzhenerno-Fizicheskii Zhurnal, Vol. 44, No. 6, pp. 988-995, June, 1983. Original article submitted March 25, 1982.

 0022-0841/83/4406-0678$07.50

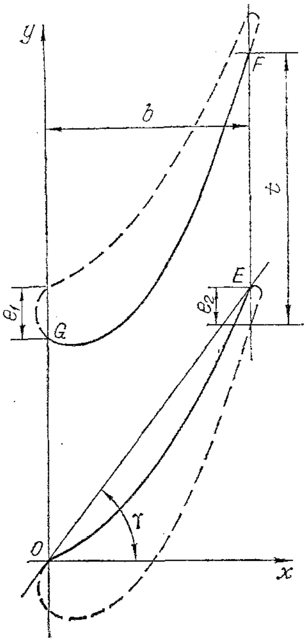

Fig. 1. Diagram of the grid.

The direction of the initial beam carrying a given portion of energy with respect to the normal to the emitting surface at the point of exit of the beam is determined by selecting a random number R_δ belonging to a uniform distribution in the interval (0, 1), according to the relation

$$\delta = (R_\delta - 0.5)\pi, \tag{5}$$

while the angle δ between the beam and the normal directed into the region OEFGO is measured from the normal. The angle between the abscissa and the beam is characterized by the relations: $\alpha = \delta$ for the boundary OG, $\alpha = \pi + \delta$ for the boundary EF, $\alpha = \pi/2 + \omega_s + \delta$ for the boundary OE, $\alpha = -(\pi/2 - \omega_b - \delta)$ for the boundary GF; the angles between the abscissa and the tangent to the convex ω_s and concave ω_b surface of the interblade channel correspond to the exit points of the beam. When the beam is incident on the side surface of the interblade channel (OE or GF), the portion of energy is assumed to be absorbed if the chosen random number $R_\varepsilon \leqslant \varepsilon$. If $R_\varepsilon > \varepsilon$, absorption does not occur, and the beam is reflected diffusely or specularly. The type of reflection is established by selection of the random number R_s. If $R_s < S$, then specular reflection occurs; otherwise, the reflection is assumed to be diffuse, and the direction of the reflected beam is determined analogously to finding α for the emitted portion of energy.

The solution of the problem reduces to tracing the path of motion of each portion of energy right up to the instant of absorption by the side walls or of departure beyond the limits of the interblade channel (crossing the boundary OG or EF) and subsequent summation of the energy received by each section of the boundary of the given region.

The basic geometric relations required to determine the parameters of the energy-bearing beams and the points at which they cross the boundaries are now given. In the general case, the beam equation is written in the form

$$y_B = x_B \operatorname{tg}\alpha + C_B. \tag{6}$$

If the portion of energy begins its motion from boundary OG at the point with ordinate y_1, then obviously $C_B = y_1$. Simultaneous solution of Eqs. (4) and (6) shows that if

$$P_b = \left(\frac{\operatorname{tg}\alpha - B_b}{2A_b}\right)^2 + \frac{C_B - C_b}{A_b} > 0 \tag{7}$$

the beam crosses the convex surface; the abscissa of the intersection point for a beam arriving from the direction of boundary OG is determined by the expression

$$x_{Bb}=\frac{\operatorname{tg}\alpha-B_b}{2A_b}-\sqrt{P_b}. \tag{8}$$

When

$$0<x_{Bb}<b, \tag{9}$$

where b is the grid width (Fig. 1), the intersection point obtained (the point of incidence of the beam) falls within the limits of the interblade channel.

The condition of beam intersection with the boundary EF corresponds to the inequality

$$b\operatorname{tg}\gamma\leqslant y_{B2}\leqslant b\operatorname{tg}\gamma+t-e_2, \tag{10}$$

where γ is the angle of installation of the profile; t, grid step; e_2, thickness of the outlet edge; y_{B2} = b tan α + C_B, ordinate of the intersection point.

If Eqs. (9) and (10) do not hold, then one of the intersection points of the beam with the concave boundary lies within the segment OE. For a beam arriving from the direction of boundary OG, the abscissa of this point is determined on the basis of Eqs. (3) and (6) by means of the expression

$$x_{BS}=\frac{\operatorname{tg}\alpha-B_S}{2A_S}+\sqrt{\left(\frac{\operatorname{tg}\alpha-B_S}{2A_S}\right)^2+\frac{C_B}{A_S}}. \tag{11}$$

For the portion of energy moving from boundary EF, $C_B = y_2 - b \tan\alpha$, where y_2 is the ordinate of the point on EF at which the beam begins. When Eq. (7) holds, this beam will intersect the convex surface of the channel at the point with abscissa

$$x_{Bb}=\frac{\operatorname{tg}\alpha-B_b}{2A_b}+\sqrt{P_b} \tag{12}$$

which belongs to segment GF when Eq. (9) holds. The possibility of intersection of the beam with boundary OG is determined by the condition

$$0\leqslant C_B\leqslant t-e_1. \tag{13}$$

If Eqs. (9) and (13) do not hold, then the beam is incident on the concave surface within the limits of the interblade channel, and the abscissa of the point of incidence is

$$x_{BS}=\frac{\operatorname{tg}\alpha-B_S}{2A_S}-\sqrt{\left(\frac{\operatorname{tg}\alpha-B_S}{2A_S}\right)^2+\frac{C_B}{A_S}}. \tag{14}$$

If the portion of energy is emitted (reflected) by the concave surface, the constant in the beam equation is determined from the formula

$$C_B=A_Sx_{BS}^2+B_Sx_{BS}-x_{BS}\operatorname{tg}\alpha, \tag{15}$$

where x_{BS} is the abscissa of the point of emission. If Eq. (7) holds, the beam intersects the convex surface, and the abscissa of the intersection point when $\alpha < \pi/2$ may expediently be determined from Eq. (8); but when $\alpha > \pi/2$ – by Eq. (12). The condition of beam intersection with the boundary OG corresponds to Eq. (13), and the condition of intersection with boundary EF corresponds to Eq. (10). If Eqs. (9), (10), and (13) do not hold, the beam is incident on the concave surface (self-irradiation of the concave surface occurs) at the point with an abscissa given by Eq. (14) when $\alpha < \pi/2$, or by Eq. (11) when $\alpha > \pi/2$.

In energy emission (reflection) by a convex surface (at the point with abscissa x_{Bb})

$$C_B=A_bx_{Bb}^2+B_bx_{Bb}+C_b-x_{Bb}\operatorname{tg}\alpha. \tag{16}$$

If Eq. (13) holds, it means that the beam passes beyond the limits of the channel through boundary OG, and if Eq. (10) holds, it leaves the channel through boundary EF. If these conditions are not satisfied, then the beam interacts with the concave surface at a point with an abscissa given by Eq. (11) if $\alpha > -\pi/2$ or Eq. (14) if $\alpha < -\pi/2$. The direction of the reflected beam in specular reflection is determined from geometric considerations.

If the incident beam is characterized by $\alpha \neq \pi/2$, then the expression for the angle of incidence (the angle between the beam and the tangent to the surface at the point of beam incidence) when the beam is incident on a convex surface (at a point with abscissa x_{Bb}) may be written in the form

$$\beta_b = \mathrm{arctg}\left[\frac{2A_b x_{Bb} + B_b - \mathrm{tg}\,\alpha}{1 + (2A_b x_{Bb} + B_b)\,\mathrm{tg}\,\alpha}\right], \tag{17}$$

and when the beam is incident on a concave surface (at a point with abscissa x_{BS}), in the form

$$\beta_S = \mathrm{arctg}\left[\frac{2A_S x_{BS} + B_S - \mathrm{tg}\,\alpha}{1 + (2A_S x_{BS} + B_S)\,\mathrm{tg}\,\alpha}\right], \tag{18}$$

when $\alpha = \pi/2$

$$\beta_b = \mathrm{arctg}\left(\frac{1}{2A_b x_{Bb} + B_b}\right);\ \beta_S = \mathrm{arctg}\left(\frac{-1}{2A_S x_{BS} + B_S}\right). \tag{19}$$

In accordance with Eqs. (17)-(19), the angle of inclination of the reflected beam in specular reflection from a convex surface is $\alpha' = \omega_b - \beta_b$ when $\beta_b < 0$ and $\alpha' = \omega_b + \beta_b - \pi$ when $\beta_b > 0$; in the case of specular reflection from a concave surface, $\alpha' = \omega_S + \beta_S + \pi$ when $\beta_S < 0$, and $\alpha' = \omega_S + \beta_S$ when $\beta_S > 0$, while $\omega_b = \arctan(2A_b x_{Bb} + B_b)$; $\omega_S = \arctan(2A_S x_{BS} + B_S)$.

The representation of the radiant energy density, taking account of its dependence on the direction, is now considered.

In a plane formulation, the energy of a specific portion of radiation Δq emitted by an area bounded by the segment Δl in the given plane may be expressed in the form

$$\Delta q = E\Delta l F(\psi)\frac{\pi}{N}, \tag{20}$$

where E is the total radiation density; $F(\psi)$, directionality function of the radiation; and $\pi/N = \Delta\psi$, plane angle corresponding to the portion of radiation.

The function $F(\psi)$ is written in the form of Fourier series

$$F(\psi) = a_0 + \sum_{i=1}^{z} a_i \cos i\psi + \sum_{i=1}^{z} b_i \sin i\psi, \tag{21}$$

where, by definition, $\psi = \frac{\pi}{2} - \delta$. The assumption $a_0 = 1/\pi$, $a_{i\geqslant 1} = 0$, $b_{i\geqslant 1} = 0$ corresponds to the condition of directional independence of the radiation density. When $a_{i\geqslant 0} = 0$, $b_1 = 1/2$, $b_{i>1} = 0$, Eq. (21) gives $F(\psi) = (1/2)\sin\psi$, which corresponds to the Lambert law (for plane radiation).

An approximate function $F(\psi)$ is constructed for the radiation flux leaving the interblade channel, on the basis of the scheme for twelve ordinates. Retaining three terms of the expansion, it is found that

$$F(\psi) = a_0 + a_1\cos\psi + a_2\cos 2\psi + a_3\cos 3\psi, \tag{22}$$

where

$$a_0 = \frac{1}{12}\left[F_1(\psi) + 2\sum_{i=2}^{6} F_i(\psi) + F_7(\psi)\right]; \tag{23}$$

$$a_1 = \frac{1}{6}\left[F_1(\psi) + \sqrt{3}F_2(\psi) + F_3(\psi) - F_5(\psi) - \sqrt{3}F_6(\psi) + F_7(\psi)\right]; \tag{24}$$

$$a_2 = \frac{1}{6}[F_1(\psi) + F_2(\psi) - F_3(\psi) - 2F_4(\psi) - F_5(\psi) + F_6(\psi) + F_7(\psi)]; \tag{25}$$

$$a_3 = \frac{1}{6}[F_1(\psi) - 2F_3(\psi) + 2F_5(\psi) - F_7(\psi)]. \tag{26}$$

The values of the function are determined for each direction (sector) of any section of the given boundary as the sum of the energy in the i-th direction per unit plane angle referred to the energy passing through the section in all possible directions

$$\underset{(1<i<7)}{F_i(\psi)} = \frac{(\Sigma\Delta q)_i}{\Sigma\Delta q}\frac{6}{\pi}, \quad F_1(\psi) = \frac{(\Sigma\Delta q)_1}{\Sigma\Delta q}\frac{12}{\pi}, \quad F_7(\psi) = \frac{(\Sigma\Delta q)_7}{\Sigma\Delta q}\frac{12}{\pi}. \tag{27}$$

The number of the sector through which the given portion of energy passes corresponds to $i' = 1 + (\pi/2 - \alpha)\pi/6$, rounded to an integer. Using Eq. (22), the directional properties of the turbine grid as a reflector of radiant energy may be investigated, and the directionality of the radiation may be taken into account in calculating the radiational interaction of neighboring coronas.

The quantity Δl in Eq. (20) depends on the character of the boundary and the number of sections into which it is divided. For the j-th section of the side boundaries of the parabolic channel, under the condition that j = 1 corresponds to the section adjacent to the ordinate, the following expression may be written:

$$\begin{aligned}\Delta l_j = \frac{1}{4A}\Bigg\{&\left(2A\frac{b}{m}j + B\right)\sqrt{4A^2\left(\frac{b}{m}j\right)^2 + 4AB\frac{b}{m}j + B^2 + 1} - \\ &-\left[2A\frac{b}{m}(j-1) + B\right]\sqrt{4A^2\left[\frac{b}{m}(j-1)\right]^2 + 4AB\frac{b}{m}(j-1) + B^2 + 1} + \\ &+\ln\frac{\sqrt{4A^2\left(\frac{b}{m}j\right)^2 + 4AB\frac{b}{m}j + B^2 + 1} + 2A\frac{b}{m}j + B}{\sqrt{4A^2\left[\frac{b}{m}(j-1)\right]^2 + 4AB\frac{b}{m}(j-1) + B^2 + 1} + 2A\frac{b}{m}(j-1) + B}\Bigg\}.\end{aligned} \tag{28}$$

An example of solving the given problem for a grid with the parameters t = 0.063 m, b = 0.048 m, e_1 = 0.0115 m, e_2 = 0.0085 m, $\gamma = 53°$, A_s = 20.4681 m^{-1}, B_s = 0.344327, A_b = 38.441 m^{-1}, B_b = −0.456023, and C_b = 0.0515 m (Fig. 1) is shown in Fig. 2, where the density of radiant fluxes is shown by curves plotted along the boundaries of the interblade channel arbitrarily chosen in the form of a rectangle. The radiation density is plotted perpendicular to the boundaries of the channel everywhere in the same scale. At the solid channel boundaries, curves of the absorbed-energy density — arrows toward the boundary — and emitted (resulting) energy — arrows away from the boundary — are shown. On the lines marking the inlet and outlet of the channel, the energy density arriving at the channel (curve outside the channel) or leaving it (curves inside the channel) is plotted. Lobe diagrams show the distribution of the energy leaving the interblade channel in directions in the half plane, estimated as the ratio of the energy transmitted in the given direction to the total energy transmitted through the given section of boundary; the segment length L corresponds to unity in the diagram. On the curves of the radiation flux density, the length L corresponds to $5\cdot10^5$ W/m². The continuous curves correspond to $\varepsilon_s = \varepsilon_b = 1$, the dashed curves to $\varepsilon_s = \varepsilon_b = 0.5$, $S_s = S_b = 0$, and the dash-dot curves to $\varepsilon_s = \varepsilon_b = 0.5$, $S_s = S_b = 1$. The calculations were performed on an M-220 computer for m = n = 5 and N = 10,000. The distribution of the energy incident on the blades from the direction of the inlet to the grid is shown in Fig. 2a; this distribution is found under the assumption that the incident-energy density is $E_{in} = 5\cdot10^5$ W/m² and does not depend on the direction, while there is no intrinsic emission of the solid channel walls. Analogous data are shown in Fig. 2b for the case when the energy is incident from the direction of the outlet from the grid $E_{out} = 5\cdot10^5$ W/m², under the condition that E_{in} and the intrinsic emission of the solid channel walls are zero. It is evident from Figs. 2a, b that energy absorption by the solid boundaries occurs mainly on sections close to the region of admission of the radiant flux. The transmissivity of the grid is smaller for E_{in} than for E_{out}; the degree of specularity of the blade surfaces forming the grid significantly influences the directionality of the energy transmitted and reflected by the grid.

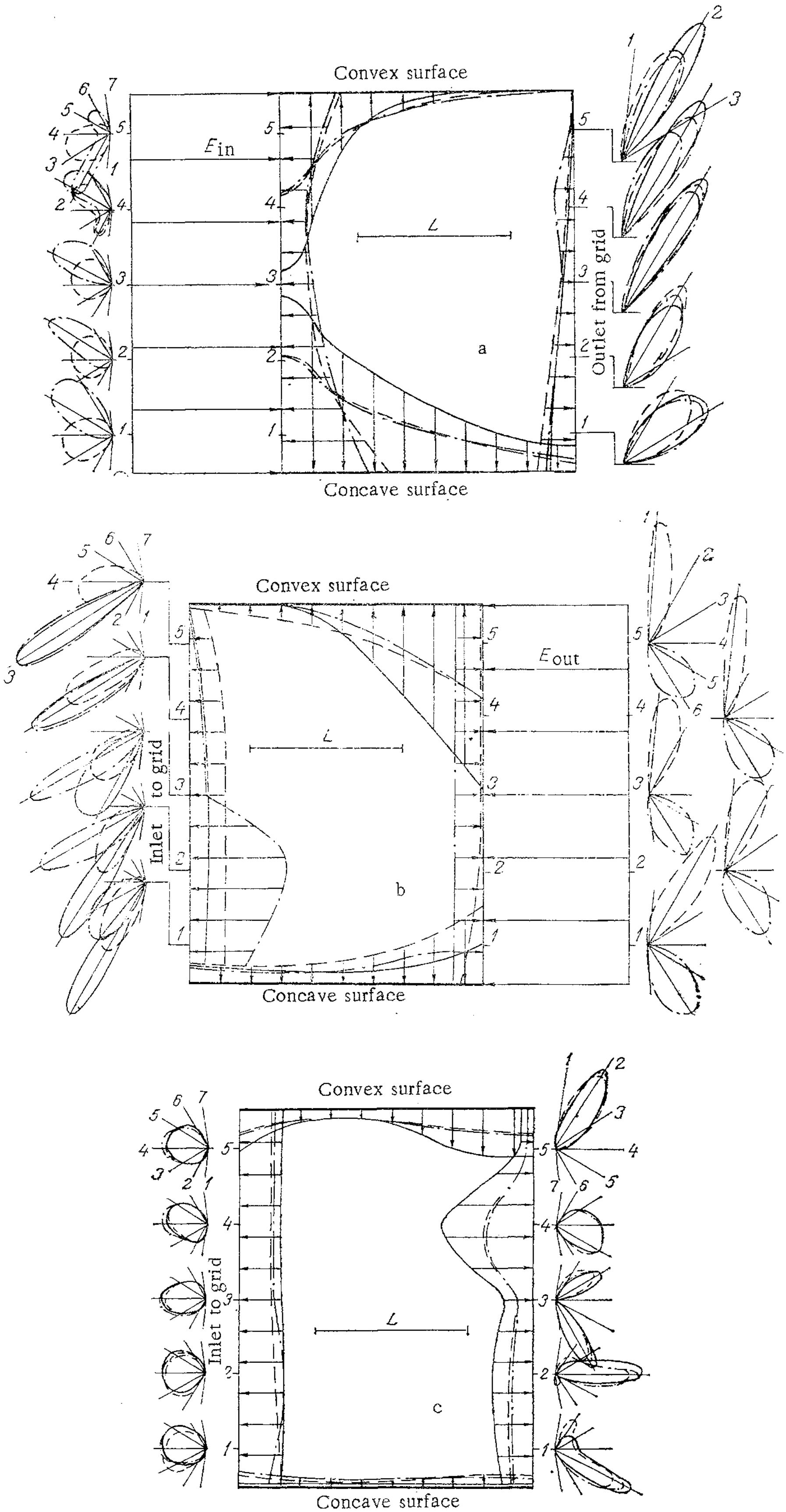

Fig. 2. Radiant-energy distribution over the interblade-channel boundary: a, b) energy directed into the grid through the inlet and outlet cross sections, respectively; c) energy emitted by the walls of the grid blades.

The distribution of the density of the resulting radiant flux of the walls $E = \varepsilon\sigma_0 T_B^4 - E_{abs}$ and the radiant energy leaving the grid are shown in Fig. 2c for $E_{in} = E_{out} = 0$ and $T_B = 1223°K$. In this case the directionality diagrams are found to be practically the same for all the given conditions.

The given data indicate the considerable nonuniformity of the distribution of radiant heat fluxes in a turbine grid, which may exert a significant influence on the thermal and thermostress state of the blades of high-temperature gas turbines. Thus, taking into account that in modern gas-turbine motors the radiation density of the combustion chamber in the combustion of kerosene is at a level of $2.5 \cdot 10^5$ W/m², the density of the radiant heat flux absorbed by the blade with a blade-surface emissivity of 0.5 is approximately $0.5 \cdot 10^5 - 1 \cdot 10^5$ W/m² in the region of the inlet edge, according to Figs. 2a, c; for typical conditions of the first stage of gas-turbine-motor turbines, this gives $\bar{E}_B = 0.05-0.1$, and hence when $\theta_{conv} = 0.5$, the cooling efficiency of the inlet edge is reduced, as a result of radiant heating, by 0.025-0.05.

NOTATION

T, temperature; θ, cooling efficiency of blade (subscript 0 denotes the value when $E_B = 0$); α_G, heat-transfer coefficient from the direction of the gas; α, β, γ, δ, ω, ψ, angles; E, radiant heat-flux density (subscript B denotes that absorbed by the blade); ε, emissivity; S, degree of specularity; R, random number; x, y, coordinates; t, grid step; e, thickness of the blade edge; A, B, C, coefficients of the parabolas describing the blade profile, constants; a_i, b_i, coefficients; F(ψ), directionality function; P, parameter; i, j, number of section, direction. Subscripts: A, air; G, gas; conv, convective; F, film; B, blade, beam; S, saddle (concave surface); b, back edge (convex surface); in, 1, inlet to the grid; out, 2, outlet from the grid; abs, absorbed.

LITERATURE CITED

1. S. Z. Kopelev and S. V. Gurov, Thermal State of Constructional Elements of Aviation Motors [in Russian], Mashinostroenie, Moscow (1978).
2. Khill and Dibelus, "Measuring the temperature and emissivity of flames in gas-turbine combustion chambers," Energet. Mash. Ustan., No. 3, 106-111 (1970).
3. Dzh. R. Khauel, "Using the Monte Carlo method in heat-transfer problems," in: Successes in Heat Transfer [Russian translation], Mir, Moscow (1971), pp. 7-67.
4. E. M. Sparrow and R. D. Sess, Radiant Heat Transfer [Russian translation], Énergiya, Leningrad (1971).